CBPF-NF-033/04

Alpha Decay Half-Life of Bismuth Isotopes*

O A P Tavares[1], E L Medeiros[1] and M L Terranova[2]

[1]Centro Brasileiro de Pesquisas Físicas - CBPF/MCT, Rua Dr. Xavier Sigaud 150, 22290-180 Rio de Janeiro-RJ, Brazil

[2]Dipartimento di Scienze e Tecnologie Chimiche, Università degli Studi di Roma "Tor Vergata", and Istituto Nazionale di Fisica Nucleare-INFN, Sezione di Roma 2, via della Ricerca Scientifica, 00133 Roma, Italy

Abstract - The observed alpha decay half-life-values of favoured alpha transitions of $\ell = 5$ in bismuth isotopes have been analyzed in the framework of a model based on the quantum mechanical tunnelling through a potential barrier where the centrifugal and overlapping effects are taken into account. In particular, the very recent measured alpha decay half-life-value of $(1.9 \pm 0.2) \times 10^{19}$ y for the unique naturally occurring ^{209}Bi isotope has been reproduced by the present approach as $(1.0 \pm 0.3) \times 10^{19}$ y. Besides, the partial alpha decay half-lives for a number of unmeasured alpha transitions of $\ell = 5$ in bismuth isotopes are predicted by the model, thus making possible to evidence the influence of the 126 neutron shell closure on the alpha decay half-life. The present approach has shown to be successfully applicable to other isotopic sequences of alpha-emitter nuclides.

*Dedicated to Prof. Cesare M.G. Lattes, one of the discoverers of the π-meson, on the occasion of his 80^{th} birthday.

1 Introduction

Bismuth, first described in 1450 by the german monk Basil Valentine, forms the only naturally occurring 209 mass number isotope, but a large number of artificially produced radioactive isotopes of mass number in the range $186 \leq A \leq 216$ are known today, most of them being unstable against alpha particle, electron capture and beta-minus decays [1]. Since the late fourties, attempts were made to detect a possible alpha activity from ^{209}Bi isotope, and results indicated half-life-values in the range $(2.0–2.7)\times10^{17}$ y [2–4], or lower limits of 3×10^{15} y [5], 2.0×10^{18} y [6,7], and 1.0×10^{19} y [8] for the alpha decay half-life.

It was only very recently that the spontaneous alpha particle emission from natural bismuth was detected unambigously for the first time by de Marcillac *et al.* [9], who developed and used the scintillating bolometer technique with massive (45.7 and 91.2 g) BGO ($Bi_4Ge_3O_{12}$) crystals for detection of the alpha particles. The measured half-life was found $(1.9 \pm 0.2) \times 10^{19}$ y, with a Q-value for decay of (3.137 ± 0.002) MeV, thus comparing quite well with the theoretical expectations [7,8].

This spectacular finding, the lowest alpha activity ever detected (~ 12 disintegrations/h·kg), motivated us to develop a simple, one-parameter model based on the quantum mechanical tunnelling mechanism of penetration through a potential barrier, as first proposed by Gamow [10], and Condon and Gurney [11]. This treatment enabled us to calculate and systematize the alpha decay half-life of ground-state to ground-state transitions of mutual angular momentum $\ell = 5$ for all alpha-emitter bismuth isotopes. The choice for $\ell = 5$ comes from the nuclear spin ($\boldsymbol{J}$) and parity (π) conservation laws ($\boldsymbol{J}_{\mathsf{p}} = \boldsymbol{J}_{\mathsf{d}} + \boldsymbol{J}_{\alpha} + \boldsymbol{\ell}$, $\pi_{\mathsf{p}} = \pi_{\mathsf{d}} \cdot \pi_{\alpha}(-1)^{\ell}$) applied to alpha transitions ($J^{\pi_\alpha}_{\alpha} = 0^+$) of bismuth isotopes. Since, for instance, $J^{\pi_{\mathsf{p}}}_{\mathsf{p}} = 9/2^-$ for the parent nucleus ^{209}Bi, and $J^{\pi_{\mathsf{d}}}_{\mathsf{d}} = 1/2^+$ for the daughter nucleus ^{205}Tl it results, therefore, in a unique possible value $\ell = 5$ for the mutual angular momentum (the same happens to other fifteen alpha decay cases of Bi isotopes [1]). The present study has shown quantitatively that the dramatically very low alpha activity observed in natural bismuth as mentioned above originates from a *minimum* in the Q-value for decay which is clearly observed at 126 neutron shell closure (i.e., in ^{209}Bi isotope) when the Q-values are plotted against neutron number of the *parent*, bismuth isotopes. On the opposite side, ^{211}Bi does exhibit a very high alpha activity (nearly 25 orders of magnitude higher than that of ^{209}Bi), for a *maximum* in the Q-value is located just on 126 neutron number of the *daughter* nucleus ^{207}Tl.

By assuming *a priori* an alpha-particle preformation probability equal to unity (this assumption will be reconsidered later, in section 2.1), a simple, semiempirical description to alpha emission from nuclei, following the classical, one-dimensional WKB-integral approximation to evaluate the penetrability through a potential barrier, has shown a practically linear relationship between the inverse square root of Q_α-value and the logarithm of the partial alpha decay half-life, $T_{1/2_\alpha}$, as usually has been obtained in systematic studies of alpha decay. This will be the subject of the next sections.

2 Semiempirical approach to alpha decay by tunnelling

According to the current, quantum mechanical theory for alpha emission from nuclei [12], the decay constant, λ, is calculated as

$$\lambda = \lambda_0 P, \quad P = \mathrm{e}^{-G}, \quad G = \frac{2}{\hbar}\int_a^b \sqrt{2\mu(s)\,[V(s) - Q_\alpha]}\,\mathrm{d}s\,, \tag{1}$$

where s is the separation between the centres of the alpha particle and daughter nucleus, $V(s)$ is the potential barrier, Q_α is the Q-value for alpha decay, $\mu(s)$ is the reduced mass of the disintegrating system, a and b are, respectively, the inner and outer turning points (see Fig. 1), G is the classical WKB-integral approximation (often called Gamow's factor for decay), P is the penetrability factor through the barrier, λ_0 is the frequency factor which represents the number of assaults on the barrier per unit of time, and $\hbar = h/2\pi$ is Planck's constant.

The quantity λ_0 is usually estimated as

$$\lambda_0 = \frac{v}{2a} = \frac{2^{1/2}}{2a}\left(\frac{Q_\alpha}{\mu_0}\right)^{1/2}, \tag{2}$$

where v is the relative velocity of the fragments, $a = R_\mathsf{p} - R_\alpha$ is the difference between the radius of the parent nucleus and the alpha-particle radius, and μ_0 is the final reduced mass of the system (see below). In addition, we have considered only those alpha decays which take place from the ground-state of the parent nucleus to the ground-state of the daughter nucleus (gs-gs transitions), for which cases the total energy available in the decay is given by the usual Q-value, i.e.

$$Q_\alpha = m_\mathsf{p} - (m_\mathsf{d} + m_\alpha)\ . \tag{3}$$

Here the m's denote the nuclear (rather than the atomic) masses of the participating nuclides (the subscripts p, d, and α refer to, respectively, the parent nucleus, daughter

nucleus, and alpha particle). Both the values of μ_0 and Q_α have been calculated from the most recent atomic mass-excess (ΔM) evaluation [13] by using the expressions

$$\frac{1}{\mu_0} = \frac{1}{m_{\mathsf{d}}} + \frac{1}{m_\alpha} \tag{4}$$

$$m_{\mathsf{d}} = A_{\mathsf{d}} + \frac{\Delta M_{\mathsf{d}}}{F} - \left(Z_{\mathsf{d}} m_{\mathsf{e}} - \frac{10^{-6} k Z_{\mathsf{d}}^{\beta}}{F} \right) \text{ u} \tag{5}$$

$$Q_\alpha = \Delta M_{\mathsf{p}} - (\Delta M_{\mathsf{d}} + \Delta M_\alpha) + 10^{-6} k \left(Z_{\mathsf{p}}^{\beta} - Z_{\mathsf{d}}^{\beta} \right) \text{ MeV}, \tag{6}$$

where $m_\alpha = 4.001506179144$ u is the alpha-particle mass, $m_{\mathsf{e}} = 0.548579911 \times 10^{-3}$ u is the electron rest mass, $F = 931.494009$ MeV/u is the mass-energy conversion factor, and $\Delta M_\alpha = 2.42498783$ MeV. The quantity kZ^β represents the total binding energy of the Z electrons in the atom, where the values of $k = 8.7$ eV and $\beta = 2.517$ have been derived from data reported by Huang *et al.* [14]. In this way, the last term in Eq. (6) represents the screening effect on the Q_α-value. Finally, by expressing lengths in fm, and time in s, the alpha decay half-life, $T_{1/2_\alpha} = \lambda^{-1} \ln 2$, is calculated as

$$T_{1/2_\alpha} = 1.0 \times 10^{-22} a \left(\frac{\mu_0}{Q_\alpha} \right)^{1/2} \mathrm{e}^{G} \text{ s}. \tag{7}$$

2.1 Gamow's factor for decay

The G-factor defined in Eq. (1) is the utmost important quantity in evaluating the half-life values. It is calculated over the entire barrier region, $a \leq s \leq b$ (Fig. 1), and is given by the sum of two components. The first one is the G-factor in the overlapping region, G_{ov}, where the alpha particle drives away from the parent nucleus until the configuration at contact is reached (the region $a \leq s \leq c$ in Fig. 1). The second component is the G-factor in the separation region, G_{se}, which extends from the contact configuration at $c = R_{\mathsf{d}} + R_\alpha$ up to the outer turning point at b, where the potential energy equals the Q_α-value, i.e., $V(b) = Q_\alpha$.

In the overlapping region both the effective reduced mass, $\mu(s)$, and the potential energy, $V(s)$, are not known exactly. Duarte and Gonçalves [15] have studied the behaviour of $\mu(s)$ for different cases of hadronic decays. For alpha particle emission from ^{222}Ra their results can be described quite well by a cubic of the form $\mu(s) = \mu_0[(s-a)/(c-a)]^3$. On the other hand, Poenaru *et al.* [16] have assumed for the potential barrier a quadratic function of the type $V(s) = Q_\alpha + (V_c - Q_\alpha)[(s-a)/(c-a)]^2$, where V_c is the potential

energy at the contact configuration. These two descriptions [15,16] have suggested us, likewise, to assume power functions in describing the variations of both $\mu(s)$ and $V(s)$ in the overlapping region, in such a way that

$$\mu(s) = \mu_0 \left(\frac{s-a}{c-a}\right)^p , \;\; p \geq 0 \, , \tag{8}$$

$$V(s) = Q_\alpha + (V_c - Q_\alpha) \left(\frac{s-a}{c-a}\right)^q , \;\; q \geq 1 \, , \tag{9}$$

with

$$V_c = \frac{2Z_{\mathsf{d}}e^2}{c} + \frac{\ell(\ell+1)\hbar^2}{2\mu_0 c^2} \, , \tag{10}$$

where $e^2 = 1.4399652$ MeV·fm is the square of the electronic elementary charge, and ℓ is the mutual orbital angular momentum resulting from the centrifugal barrier associated with the rotation of the disintegration product nuclei around their common centre of mass. Accordingly, the calculation of G_{ov} gives

$$G_{\mathsf{ov}} = 0.4374702(c-a)g \left\{ \mu_0 \left[\frac{2Z_{\mathsf{d}}e^2}{c} + \frac{20.9008\,\ell\,(\ell+1)}{\mu_0 c^2} - Q_\alpha \right] \right\}^{1/2} , \tag{11}$$

where

$$g = \left(1 + \frac{p+q}{2}\right)^{-1} , \;\; 0 < g \leq 2/3 \tag{12}$$

is the adjustable parameter of the model, the value of which being thus determined from a set of measured half-life values (see below).

The calculation of G_{se}, including the centrifugal term to the potential barrier, has been done elsewhere [17], and the result reads

$$\begin{aligned} G_{\mathsf{se}} \;\; = \;\; & 1.25988372 Z_{\mathsf{d}} \left(\frac{\mu_0}{Q_\alpha}\right)^{1/2} \left\{ \frac{x^{1/2}}{2y} \times \ln \frac{\left[x\,(x+2y-1)\right]^{1/2} + x + y}{\frac{x}{y}\left[1 + \left(1 + \frac{x}{y^2}\right)^{1/2}\right]^{-1} + y} + \right. \\ & \left. + \arccos \left\{ \frac{1}{2}\left[1 - \frac{1 - \frac{1}{y}}{\left(1 + \frac{x}{y^2}\right)^{1/2}}\right] \right\}^{1/2} - \left[\frac{1}{2y}\left(1 + \frac{x}{2y} - \frac{1}{2y}\right)\right]^{1/2} \right\} , \end{aligned} \tag{13}$$

where

$$x = \frac{20.9008\,\ell(\ell+1)}{\mu_0 c^2 Q_\alpha} , \;\; y = \frac{Z_{\mathsf{d}}e^2}{cQ_\alpha} \, . \tag{14}$$

Figure 1 shows the potential energy barrier for the two extreme cases (in half-life values) of alpha emission occurring in ^{187}Bi (bottom) and ^{209}Bi (top) isotopes, where the various quantities mentioned in the description above are made clear (bottom of Fig. 1). Both cases are for $\ell = 5$, and they differ from each other by ~ 27 orders of magnitude in the half-life. The Coulomb potential is shown by dotted lines.

At this point, it is worthwhile to mention that according to a much modern description to alpha and cluster decays [18,19], Eq. (1) can be rewritten as

$$\lambda = \lambda_0 S_\alpha P_{\mathsf{se}} \,, \;\; S_\alpha = \mathrm{e}^{-G_{\mathsf{ov}}} \,, \;\; P_{\mathsf{se}} = \mathrm{e}^{-G_{\mathsf{se}}} \,, \tag{15}$$

where S_α is the alpha particle preformation probability at the nuclear surface (also known as spectroscopic factor). We can, therefore, interpret the quantity $P_{\mathsf{se}} = \mathrm{e}^{-G_{\mathsf{se}}}$ as the penetrability factor through the external barrier region ($c \leq s \leq b$ in Fig. 1) (as in fact it is), at the same time that the quantity $S_\alpha = \mathrm{e}^{-G_{\mathsf{ov}}}$ ($S_\alpha < 1$) is being given by the penetrability factor through the overlapping region of the barrier (Fig. 1). In this way, S_α would correspond to the "arrival" of the alpha particle at the nuclear surface [19], i.e. the alpha particle preformation probability.

2.2 Nuclear radii

The penetrability factors $\mathrm{e}^{-G_{\mathsf{ov}}}$ and $\mathrm{e}^{-G_{\mathsf{se}}}$ are not strongly dependent upon the Q_α-values only, but they are also largely affected by the choice made for the nuclear radii of the parent and daughter nuclides and the alpha-particle radius as well, especially in the calculation of $\mathrm{e}^{-G_{\mathsf{se}}}$. To begin with, in a previous work devoted to systematization of 174 measured alpha-decay half-life values for even-even alpha emitter nuclides covering the mass number interval $106 \leq A \leq 264$ [20], the value $R_\alpha = (1.62 \pm 0.01)$ fm was adopted for the equivalent sharp radius of the alpha particle. This radius-value comes from the charge density distribution resulting from data on elastic electron scattering from ^{4}He as measured by Sick *et al.* [21]. Excellent reproductivity of the data was attained by using the above R_α-value coupled with a simple, Gamow-like model where, in addition, nuclear deformation effects were included, and without using any adjustable parameter [20]. For this reason, we decided to adopt the *a priori* same value of $R_\alpha = (1.62 \pm 0.01)$ fm in the present analysis.

Finally, we found from the droplet model of atomic nuclei [22,23] a good estimation of nuclear radii for the parent, R_{p}, and daughter, R_{d}, nuclei, which is consistent with the limiting conditions defined for parameter g (Eq. (12)). Accordingly, preliminary

calculations have indicated the average equivalent root-mean-square radius of the nucleon density distribution as the best choice for R_{p} and R_{d}. These have been thus evaluated as

$$R_i = \frac{Z_i}{A_i} R_{pi} + \left(1 - \frac{Z_i}{A_i}\right) R_{ni} \ , \quad i = \mathsf{p}, \mathsf{d} \ , \tag{16}$$

where the R's are given by

$$R_{ji} = r_{ji} \left[1 + \frac{5}{2}\left(\frac{w}{r_{ji}}\right)^2\right] \ , \quad j = p, n \, ; \quad i = \mathsf{p}, \mathsf{d} \ , \tag{17}$$

in which $w = 1$ fm is the diffuseness of the nuclear surface, and the r's represent the equivalent sharp radius of the proton ($j = p$) or neutron ($j = n$) density distribution. These latter quantities, in turn, are calculated following the Finite-Range Droplet Model description of nuclei by Möller *et al.* [23], thus giving

$$r_{pi} = r_0 \left(1 + \overline{\epsilon_i}\right) \left[1 - \frac{2}{3}\left(1 - \frac{Z_i}{A_i}\right)\left(1 - \frac{2Z_i}{A_i} - \overline{\delta_i}\right)\right] A_i^{1/3}, \tag{18}$$

$$r_{ni} = r_0 \left(1 + \overline{\epsilon_i}\right) \left[1 + \frac{2}{3}\frac{Z_i}{A_i}\left(1 - \frac{2Z_i}{A_i} - \overline{\delta_i}\right)\right] A_i^{1/3}, \tag{19}$$

where

$$\overline{\epsilon_i} = \frac{1}{4\,\mathrm{e}^{0.831 A_i^{1/3}}} - \frac{0.191}{A_i^{1/3}} + \frac{0.0031 Z_i^2}{A_i^{4/3}} \ , \tag{20}$$

$$\overline{\delta_i} = \left(1 - \frac{2Z_i}{A_i} + 0.004781 \frac{Z_i}{A_i^{2/3}}\right) \Bigg/ \left(1 + \frac{2.52114}{A_i^{1/3}}\right) \ , \tag{21}$$

$r_0 = 1.16$ fm, and, as before, $i = \mathsf{p}$ (parent) or d (daughter). Formulas (16)–(21) give for the nuclear radius parameter $r_{0i} = R_i/A_i^{1/3} (i = \mathsf{p}, \mathsf{d})$ of the equivalent liquid drop model values in the range 1.212–1.214 fm, which compare rather well to other $R/A^{1/3}$-evaluations [24,25] for complex nuclei in the mass region $180 < A < 220$. The R_{p}- and R_{d}-values calculated as explained above have shown to work quite satisfactorily when applied to the alpha-decay systematics of bismuth isotopes.

3 Results and discussion

According to the nuclear spin and parity conservation laws we identified twenty one cases of ground-state to ground-state alpha transitions of $\ell = 5$ among the bismuth isotopes [26]. In two cases (^{202,208}Bi), ℓ can take the values 3, 5 and 7. In another two cases (^{204,206}Bi), ℓ can take the values 5 and 7, and in only one case (^{200}Bi), the values 5, 7

and 9 are possible. In all these cases, we have assigned the value $\ell = 5$. In addition, seven of all the twenty one alpha-decay cases have indication of total half-life and alpha-decay branching ratio (three first columns in Table 1), therefore their partial alpha decay half-lives are known (6^{th} column in Table 1). By using these data as input to the present semiempirical model we found the value of the adjustable parameter, g, by minimizing the quantity

$$\sigma = \left\{ \frac{1}{5} \sum_{i=1}^{7} \left[\log_{10} \left(\frac{T^{\mathsf{e}}_{1/2_i}}{T^{\mathsf{c}}_{1/2_i}} \right) \right]^2 \right\}^{1/2} , \tag{22}$$

thus obtaining $g = 0.3846$ with $\sigma_{\min} = 0.242$ (see Fig. 2). This g-value was then used back into the routine calculation of the model to obtain the partial alpha decay half-life values for all the twenty one bismuth isotopes (7^{th} column in Table 1). It is worthwhile to note that the calculated half-life so obtained for ^{209}Bi isotope, $(1.0 \pm 0.3) \times 10^{19}$ y, differs from the novel, measured value $(1.9 \pm 0.2) \times 10^{19}$ y [9] by only a factor ~ 2. Good reproducibility is also found for the other seven bismuth isotopes, as one can appreciate from inspection on Table 1 (8^{th} column). It is remarkable that in the cases for ^{193,212,214}Bi isotopes the agreement between calculated and experimental results is particularly quite excellent ($\lesssim 15\%$). It should be noted that the screening to the nucleus caused by the surrounding electrons (represented by the last term in Eq. (6)) amounts to 35 keV for all alpha decay cases investigated here. We calculate the change in partial alpha decay half-life when the present model is used with and without the screening term. In the case of ^{209}Bi alpha decay, for which case a major effect due to screening should be expected, the exclusion of the screening term in the Q_α-value evaluation causes an increasing in the calculated half-life by a factor ~ 2.7 only. Such a change in the half-life may, however, be compensated by a little change in the value of parameter g (estimated in $\sim -10\%$). Accordingly, we decided to include the screening effect throughout the present systematic study. Finally, Table 1 shows also the resulting values for the alpha particle preformation probability, $S_\alpha = \mathrm{e}^{-G_{\mathsf{ov}}}$ (5th column), which values appear quite reasonable ones.

Figure 3 shows the dependence of partial alpha decay half-life (circles) upon $Q_\alpha^{-1/2}$ from data listed in Table 1. A trend very close to a linear one (in log-scale) is apparent, as usually has happened in other alpha-decay systematic studies [27]. The trend depicted in Fig. 3 for bismuth isotopes does indicate a strong correlation between the half-life and the energy available for decay, resembling a Geiger-Nuttall-like law of old times [28], meaning that the Q_α-value is indeed the main quantity which gives the strength of the

alpha activity of an isotopic sequence. Similar results have also been obtained when the present model is applied to other isotopic sequences such as those reported in Fig. 3. But the Q_α-value depends ultimately on detailed pairing and shell structure effects, which we shall not discuss here.

Another insight related to the results for the bismuth isotopes is represented in Fig. 4, where the behaviour of partial alpha decay half-life (Fig. 4-c) is seen as a perfect inverse reflection of the Q_α-value (Fig. 4-a) when both these quantities are plotted against neutron number of thallium isotopes. Here, the influence of the 126-neutron shell closure, which in turn is manifested on the Q_α-value, is clearly evidenced, thus making ^{211}Bi isotope much more alpha active than its neighboring isotopes, particularly ^{209}Bi isotope, which exhibit practically the highest half-life.

It is very interesting to note that the calculated preformation probability factor $S_\alpha = \mathrm{e}^{-G_{\mathsf{ov}}}$ (Fig. 4-b) exhibits the same trend as the Q_α-value does. This is because both the quantities μ_0 and $c - a$ in Eq. (12) are practically constant for bismuth isotopes, at the same time that the quantity c does not vary significantly (less than 4%) in the mass range $183 \leq A_{\mathsf{d}} \leq 210$. Consequently, the values of S_α are basically affected by the corresponding Q_α-values. In addition, since the variation of S_α for bismuth alpha emitter isotopes is only of the order of $\sim 50\%$, the conclusion can be drawn that the partial alpha decay half-life-values are dictated mainly by the penetrability factor $P_{\mathsf{se}} = \mathrm{e}^{-G_{\mathsf{se}}}$ associated with the Coulomb-plus-centrifugal potential barrier in the separation region. But this latter quantity depends, in turn, very strongly upon Q_α-value, so does the $T_{1/2_\alpha}$-values.

4 Summary and conclusion

Motivated by the very recent experimental determination of the alpha radioactivity in natural bismuth (^{209}Bi isotope), amounting to a value as low as 12 disintegrations/h·kg [9], we have developed a one-parameter, semiempirical model to analyze in a systematic way the measured alpha decay half-lives of bismuth isotopes, and to make, in addition, predictions for a number of decay cases experimentally unaccessible. We have considered all the twenty one bismuth isotopes which produce ground-state to ground-state transitions with orbital angular momentum of $\ell = 5$.

The present model has been constructed under the following basic assumptions: i) the decaying system oscillates with a frequence $\lambda_0 \approx 2 \times 10^{21}$ s^{-1}, which represents the

number of attempts per second to penetrate a potential barrier by the quantum mechanical tunnelling effect; ii) the entire Q_α-value for decay is the effective total disintegration energy of the system available for the two-body relative-motion channel; the Q_α-value has been calculated from the nuclear (rather than the atomic) mass values of the participating nuclides, therefore, taking into account screening effects; iii) the potential barrier is composed of a nuclear, overlapping region where the disintegration products (alpha particle and daughter nucleus) are drawing out from each other, and of an external, separation region extending from the configuration at contact of fragments up to the point at which the potential energy equals the Q_α-value; the penetrability through the inner part of the potential is considered to represent the alpha particle preformation probability; the external barrier is the sum of the Coulomb plus centrifugal potential barrier contributions; iv) the penetrability factor through the barrier is calculated by the usual, one-dimensional WKB-integral approximation; v) the interacting fragments are considered to be spherical, and the radii of the parent and daughter nuclei are given by their average equivalent root-mean-square radius-values of the nucleon density distribution following the Finite-Range Droplet Model parametrization by Möller *et al.* [23]; the value of alpha-particle radius is set equal to (1.62 ± 0.01) fm, as it comes from electron scattering experiments on ^{4}He [21]; vi) the adjustable parameter of the model, g, emerges from a simple description for the overlapping barrier region, and its value is determined from known (seven decay cases) experimental partial alpha decay half-lives.

In this way one calculates the alpha half-lives for a number of decay cases of bismuth isotopes, and one compares the results with the experimental ones. It is verified that the measured partial alpha decay half-life values are reproduced by the above method within a factor ~ 2 (in a few cases within 15%). This result can, to our view, be considered rather satisfactory if one looks over the extension of 24 orders of magnitude covered by the half-lives. The present analysis enables us to conclude that a strong, direct dependence of the half-life upon Q_α-value, and ultimately upon the detailed pairing plus shell effects presented by the participating nuclides, is clearly evidenced, and particularly observed in the vicinity of the 126 neutron shell structure of the parent or daughter nuclei. Shell effects are also clearly manifested in the alpha particle preformation probability factor. Finally, we have extended the above semiempirical, analytical procedure to other isotopic sequences such as for Dy-, Hf-, Os-, Pt-, Rn- and Cf-isotopes (Fig. 3) giving as well excellent, very close to linear correlations between $\log T_{1/2_\alpha}$ and $Q_\alpha^{-1/2}$. We believe that the present approach can provide reliable half-life predictions for novel, extremely rare

alpha-decay cases.

References

[1] G. Audi, O. Bersillon, J. Blachot, and A.H. Wapstra, Nucl. Phys. **A729**, 3 (2003).

[2] W. Riezler and W. Porschen, Z. Naturforchun. **7a**, 634 (1952).

[3] W. Porschen and W. Riezler, Z. Naturforchun. **11a**, 143 (1956).

[4] H. Faraggi and A. Berthelot, Comp. Rend. Acad. Scienc. **232**, 2093 (1951).

[5] K. Jenkner and E. Broda, Nature **164**, 412 (1949).

[6] E.P. Hincks and C.H. Millar, Proc. Roy. Soc. Can. **46**, 143 (1952).

[7] E.P. Hincks and C.H. Millar, Can. J. Phys. **36**, 231 (1958).

[8] H.G. de Carvalho and M. de Araújo Penna, Nuovo Cimento Letter **3**, 720 (1972).

[9] P. de Marcillac, N. Coron, G. Dambier, J. Leblanc, and J.P. Moalic, Nature **422**, 876 (2003).

[10] G. Gamow, Z. Phys. **51**, 204 (1928).

[11] E.U. Condon and R.W. Gurney, Nature **122**, 439 (1928); Phys. Rev. **33**, 127 (1929).

[12] P. Marmier and E. Sheldon, in Physics of Nuclei and Particles, vol. I (Academic Press, New York, 1969), page 303.

[13] G. Audi, A.H. Wapstra, and C. Thibault, Nucl. Phys. **A729**, 337 (2003).

[14] K.-N. Huang, M. Aoyagi, M.H. Chen, B. Crasemann, and H. Mark, At. Data Nucl. Data Tables **18**, 243 (1976).

[15] S.B. Duarte and M.G. Gonçalves, Phys. Rev. C **53**, 2309 (1996).

[16] D.N. Poenaru, M. Ivascu, A. Sãndulescu, and Walter Greiner, Phys. Rev. C **32**, 572 (1985).

[17] H.G. de Carvalho, J.B. Martins, and O.A.P. Tavares, Phys. Rev. C **34**, 2261 (1986).

[18] R. Blendowske, T. Fliessbach, and H. Walliser, Nucl. Phys. **A464**, 75 (1987).

[19] D.N. Poenaru and W. Greiner, Phys. Scripta **44**, 427 (1991).

[20] F. García, O. Rodríguez, M. Gonçalves, S.B. Duarte, O.A.P. Tavares, and F. Guzman, J. Phys. G: Nucl. Part. Phys. **26**, 755 (2000).

[21] I. Sick, J.S. McCarthy, and R.R. Whitney, Phys. Lett. B **64**, 33 (1976).

[22] W.D. Myers, in Droplet Model of Atomic Nuclei (Plenum, New York, 1977).

[23] P. Möller, J.R. Nix, W.D. Myers, and W.J. Swiatecki, At. Data Nucl. Data Tables **59**, 185 (1995).

[24] I. Angeli, International Nuclear Data Committee-INDC (HUN)-033, IAEA-NDS (1999).

[25] J. Dobaczewski, W. Nazarewicz, and T.R. Werner, Z. Phys. A **354**, 27 (1996).

[26] R.B. Firestone, in Table of Isotopes (8^{th} Edition), vol. II, (John Willey, New York, 1996).

[27] B.A. Brown, Phys. Rev. C **46**, 811 (1992).

[28] H. Geiger and J.M. Nuttall, Philos. Mag. **22**, 613 (1911); H. Geiger, Z. Phys. **8**, 45 (1921).

Table 1: Comparison between calculated and experimental partial alpha-decay half-lives for bismuth isotopes

Mass number A	Total half-life $T_{1/2}$(s)	Branching ratio $b_\alpha(\%)$	Q_α-value[a] (MeV)	$S_\alpha\,(10^{-3})$[b]	Partial alpha decay half-life-values[d] Experimental $T^{e}_{1/2}$ (s)	Calculated $T^{c}_{1/2}$ (s)	Difference $\log_{10}(T^{c}_{1/2}/T^{e}_{1/2})$
187	3.2×10^{-2}	———	7.824	7.00	———	1.87×10^{-1}	———
189	6.74×10^{-1}	———	7.310	6.66	———	0.75×10^{1}	———
191	1.23×10^{1}	1.74	6.814	6.35	7.07×10^{2}	4.04×10^{2}	−0.243
193	6.7×10^{1}	0.21	6.339	6.07	3.19×10^{4}	2.87×10^{4}	−0.046
195	1.83×10^{2}	0.003	5.867	5.80	6.10×10^{6}	3.38×10^{6}	−0.256
197	5.58×10^{2}	———	5.242	5.46	———	5.27×10^{9}	———
199	1.62×10^{3}	———	4.967	5.34	———	2.00×10^{11}	———
200	2.184×10^{3}	———	4.737	5.22	———	5.55×10^{12}	———
201	6.48×10^{3}	———	4.535	5.13	———	1.26×10^{14}	———
202	6.192×10^{3}	———	4.367	5.05	———	2.00×10^{15}	———
203	4.234×10^{4}	———	4.129	4.94	———	1.36×10^{17}	———
204	4.039×10^{4}	———	3.991	4.89	———	1.85×10^{18}	———
205	1.323×10^{6}	———	3.730	4.77	———	3.98×10^{20}	———
206	5.394×10^{5}	———	3.565	4.70	———	1.59×10^{22}	———
207	1.038×10^{9}	———	3.317	4.60	———	0.70×10^{25}	———
208	1.161×10^{13}	———	3.086	4.50	———	3.91×10^{27}	———
209	———	———	3.172	4.56	6.0×10^{26}[c]	3.22×10^{26}	−0.270
211	1.284×10^{2}	83.54	6.786	6.81	1.54×10^{2}	2.27×10^{2}	0.169
212	3.633×10^{3}	9.75	6.242	6.43	3.73×10^{4}	3.40×10^{4}	−0.039
213	2.735×10^{3}	1.94	6.017	6.29	1.41×10^{5}	3.25×10^{5}	0.363
214	1.194×10^{3}	0.00823	5.656	6.06	1.45×10^{7}	1.66×10^{7}	0.058

a) From nuclear mass-values (see Eqs. (3) and (6)), i.e. with screening.

b) Alpha particle preformation probability as defined in Eq. (15).

c) Ref. [9].

d) These are referred to ground-state to ground-state alpha transitions of mutual orbital angular momentum $\ell = 5$.

Figure Captions

Fig. 1 - Shape of the one-dimensional potential barrier for two alpha decaying systems. The shaded area emphasizes the overlapping separation region a–c. In the external region c–b the curve (full line) comprises superposition of the Coulomb (dotted line) and centrifugal potential barriers.

Fig. 2 - Minimization of the standard deviation σ (Eq. (22)) to determine the best value of the adjustable parameter of the model, g (Eqs. (11) and (12)).

Fig. 3 - Partial half-life, $T_{1/2_\alpha}$, plotted against $Q_\alpha^{-1/2}$ of ground-state to ground-state alpha transitions of $\ell = 5$ for twenty one alpha-active bismuth isotopes (circles); points are from data in Table 1, and the line is the trend obtained by least-squares fitting of the calculated (open circles) $T_{1/2_\alpha}$-values. Also shown are the trends obtained for different isotopic sequences of alpha-emitter nuclides (alpha transitions of $\ell = 0$) as indicated near the lines; full symbols represent experimental data [1,26], open ones are calculated $T_{1/2_\alpha}$-values from the present model, and the lines are least-squares fits to calculated values.

Fig. 4 - Q_α-value (a), preformation probability, S_α (b), and partial alpha decay half-life, $T_{1/2_\alpha}$ (c), plotted against neutron number of thallium isotopes. Points (connected by lines) represent data in Table 1: ■, calculated Q_α-values; ▲, calculated S_α-values; ●, experimental, and ○, calculated $T_{1/2_\alpha}$-values.

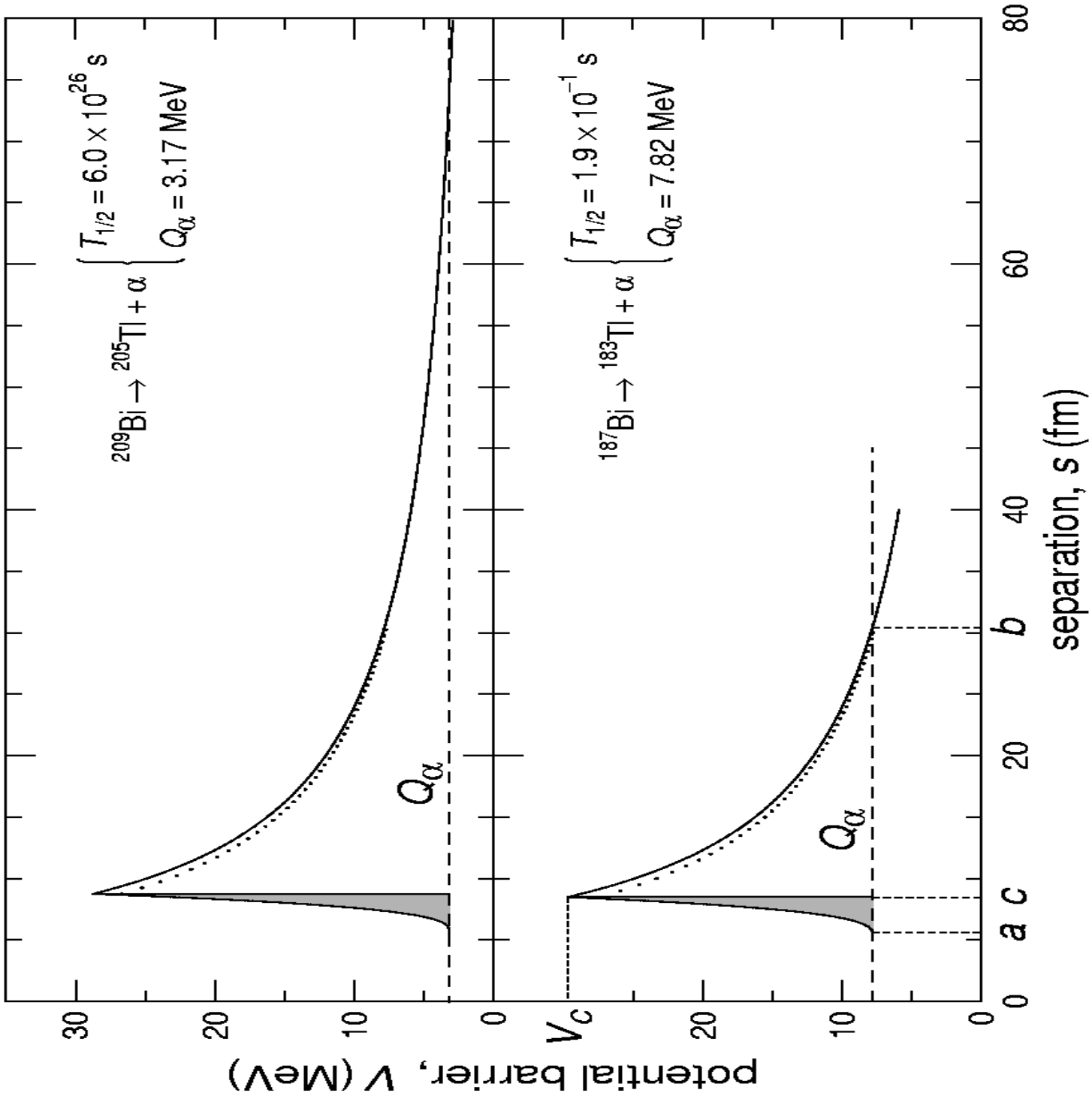
$^{209}Bi \rightarrow {}^{205}Tl + \alpha$
$T_{1/2} = 6.0 \times 10^{26}$ s
$Q_\alpha = 3.17$ MeV
$^{187}Bi \rightarrow {}^{183}Tl + \alpha$
$T_{1/2} = 1.9 \times 10^{-1}$ s
$Q_\alpha = 7.82$ MeV
Q_α
V_c
potential barrier, V (MeV)
separation, s (fm)
a c
b
0
10
20
30
40
60
80

Fig. 1

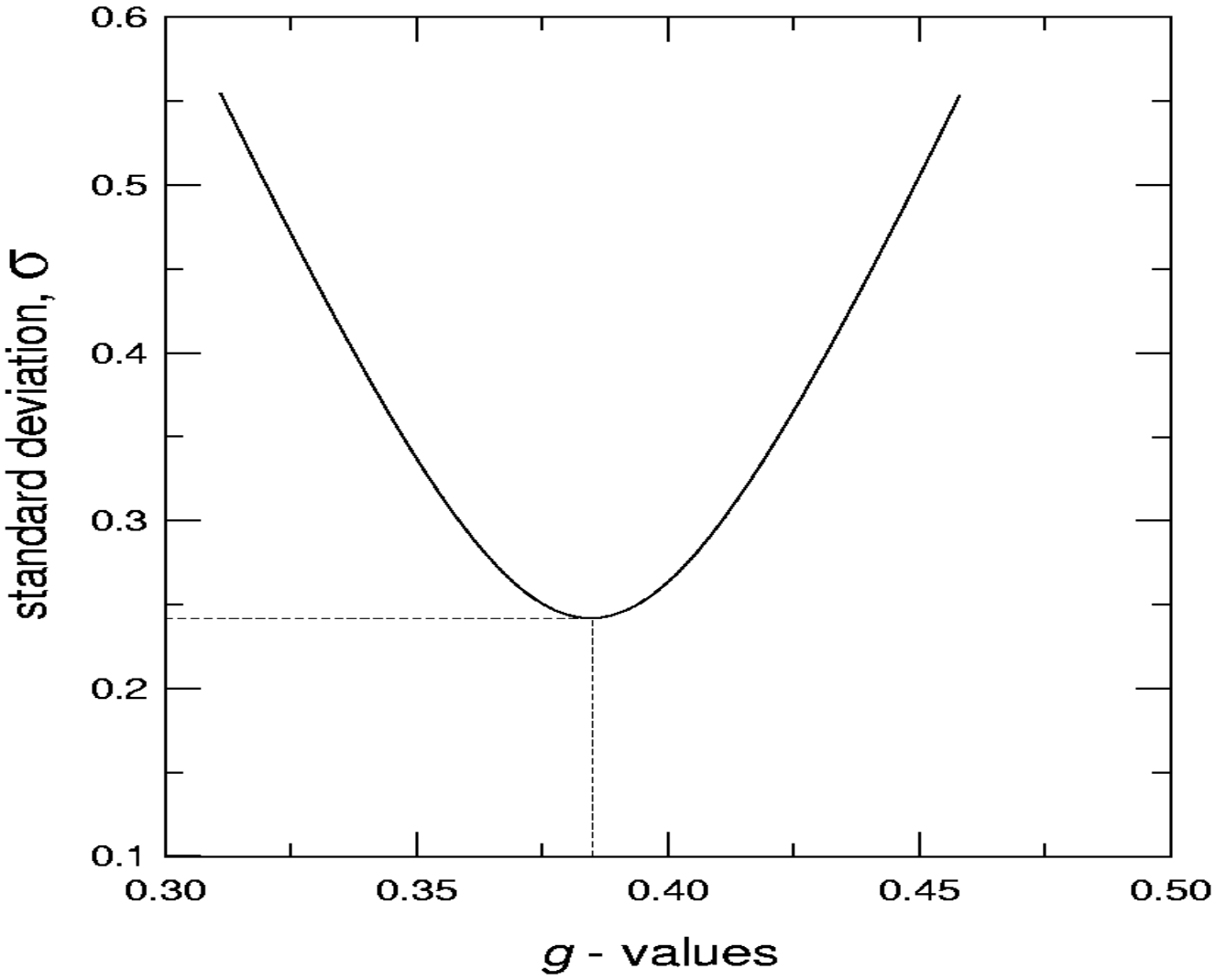
0.6
0.5
0.4
0.3
0.2
0.1
standard deviation, σ
0.30
0.35
0.40
0.45
0.50
g - values

Fig. 2

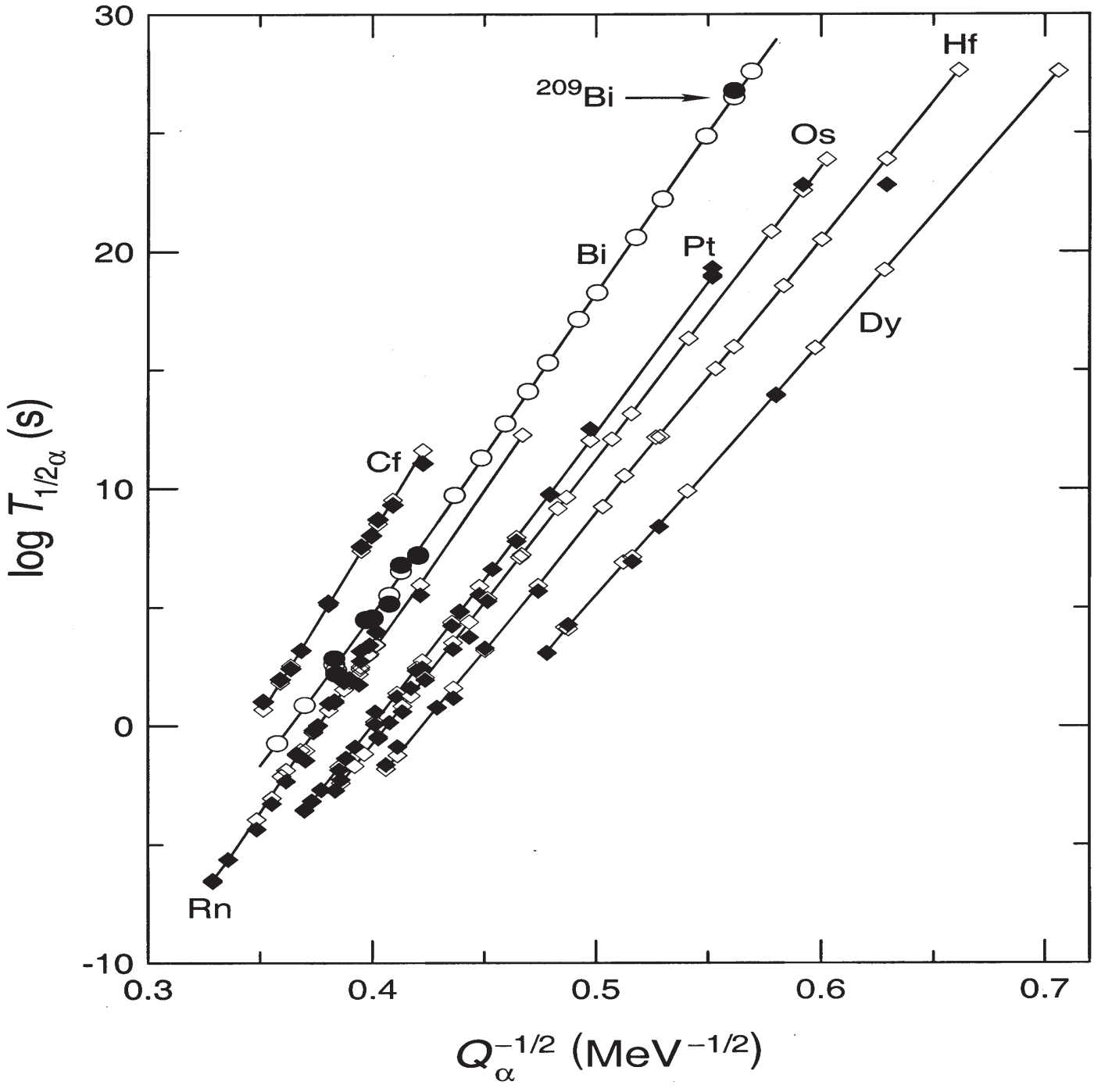
30
20
10
0
-10
0.3
0.4
0.5
0.6
0.7
log $T_{1/2\alpha}$ (s)
$Q_\alpha^{-1/2}$ (MeV$^{-1/2}$)
^{209}Bi
Hf
Os
Bi
Pt
Dy
Cf
Rn

Fig. 3

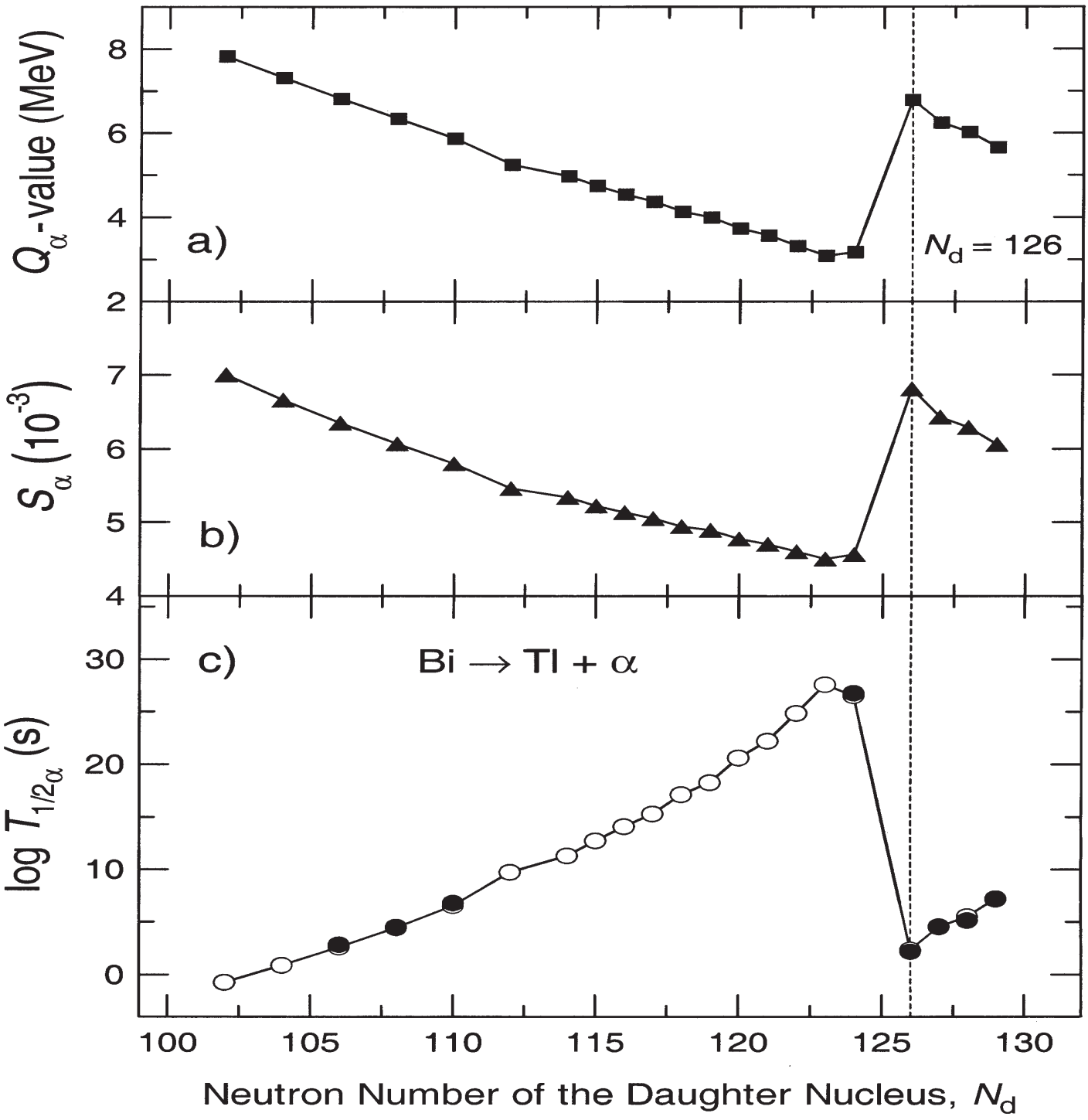
Q_α-value (MeV)
a)
N_d = 126
S_α (10^{-3})
b)
c)
Bi → Tl + α
log $T_{1/2\alpha}$ (s)
Neutron Number of the Daughter Nucleus, N_d

Fig. 4